Global Analysis of Fluorometric Titration Curves in the Presence of Excited-State Association and Quenching

Eugene Novikov[†] **and Noël Boens***[,‡]

Service Bioinformatique, Institut Curie, 26 Rue d'Ulm, Paris Cedex 05, 75248 France, and Department of Chemistry, Katholieke Universiteit Leuven, Celestijnenlaan 200F, Bus 02404, 3001 Heverlee, Belgium

Received: February 5, 2007; In Final Form: May 4, 2007

The fluorometric determination of the ground-state dissociation constant K_d of a complex between ligand and titrant with 1:1 stoichiometry in the presence of excited-state association and quenching is discussed. This report extends the results of a previous study (Novikov, E.; Stobiecka, A.; Boens, N. *J. Phys. Chem. A* **2000**, *104*, 5388), where the direct parametric fit of the fluorometric titration was used to recover reliable estimates for K_d. Here, we show that in the presence of excited-state association and quenching the unique value of K_d can be obtained from global analysis of four fluorometric titration curves measured at two emission wavelengths and two excitation wavelengths. The same identifiability criterion is applicable for systems where quenching can be neglected. The linked parameters in the global analysis are rational functions of the rate constants, independent of the excitation and emission wavelengths. The developed algorithms for the global parametric fit of fluorometric titration curves are explored using simulations.

1. Introduction

Fluorometric titration provides a powerful methodology to determine the ground-state dissociation constant K_d of host−guest complexes.[1] The advantages of fluorescence over absorption measurements are well documented[2,3] and include higher sensitivity (because fluorescence is detected vs a dark background) and selectivity (one may avoid the signal from other absorbing molecules). Furthermore, less fluorescent ligand is required in fluorometry than in spectrophotometry to attain a similar signal-to-noise ratio. Consequently, fluorometry generally produces less disturbance of the system under investigation and allows less soluble ligands to be used. Finally, fluorescence can also be used with samples of high turbidity.

Because the measured fluorescence signal F is generally dependent on excited-state and ground-state parameters (see, for example, eq 6), one can expect possible interference of the excited-state association on the fluorometric determination of the ground-state dissociation constant K_d. The potential misevaluation of K_d from fluorometric titrations can be assessed by concomitant time-resolved fluorescence measurements.[4] The fact that excited-state association can distort the K_d value estimated from fluorescence measurements is generally not well recognized, and commonly used equations for the determination of K_d from fluorometric titrations do not take into account the existence of the excited-state association reaction.[5] As was shown in ref 1, the presence of an excited-state association between ligand and titrant may yield very complicated fluorometric titration curves. The positions of the inflection points of these curves do not generally contain information that can be directly used for the determination of K_d. Moreover, the determination of the positions of inflection points (which requires numerical second-order differentiation of noisy fluorescence data) of a titration curve is unreliable because of statistical noise inherently present in the measured data and the generally very limited number of experimental points. In ref 1, we showed that the interference of the excited-state association can be eliminated by proper experimental design, i.e., by monitoring the fluorescence at the isoemissive point. This procedure can be performed at any excitation wavelength different from the isosbestic point.[6] Under this experimental condition, the uncorrupted value of K_d will be obtained from the unique inflection point of the titration curve.

In ref 7, we derived the equations relating the measured fluorescence signal F to the concentration [M] of a titrant in the presence and absence of the excited-state association with 1:n stoichiometry between ligand and titrant. We also explored the possibility to determine the correct K_d value via direct parametric fit of the fluorometric titration curve. It was shown that in the presence of excited-state association, the parametric fit of a single titration curve yields two admissible values for K_d (as roots of a quadratic equation) which cannot be distinguished without additional information. However, if the rate constants describing the excited-state processes can be estimated from independent time-resolved fluorescence measurements, the procedure leads to the unique determination of K_d.

In this paper, we extend the capability of direct parametric fit and explore the possibility to determine the *unique* value of K_d from global analysis (global parametric fit) of fluorometric titration curves measured at different excitation and emission wavelengths. We shall derive the experimental conditions, under which the unique value of K_d can be obtained, for the system with 1:1 stoichiometry of association between the ligand and titrant in the presence of excited-state association and quenching.

As in refs 1 and 7, we use the terminology and methodology of compartmental modeling to derive the expressions for the steady-state fluorescence.[8] Compartmental analysis not only provides a straightforward method to these expressions (by using matrix formalism) but also allows one to clearly specify the

* Corresponding author. Fax: +32 16 327990. E-mail: Noel.Boens@chem.kuleuven.be (N. Boens).
[†] Institut Curie.
[‡] Katholieke Universiteit Leuven.

10.1021/jp070992w CCC: $37.00
Published on Web 06/19/2007

SCHEME 1: Representation of the Kinetic Model for Intermolecular Association between Ligand and Titrant (Stoichiometry 1:1) and Corresponding Dissociation of the Formed Complex in the Presence of Quenching of the Excited States

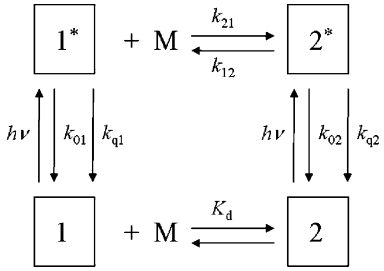

contributions of excitation, emission, and excited-state kinetics to the steady-state fluorescence signal F.

2. Steady-State Fluorescence

Consider a dynamic, linear, time-invariant, intermolecular system consisting of two distinct types of ground-state species (**1** and **2**) and two corresponding excited-state species (**1*** and **2***) as depicted in Scheme 1. Ground-state species **1** can undergo a reversible association reaction with M to form ground-state species **2**. In Scheme 1, a 1:1 stoichiometry between species **1** and M is assumed. It is further understood that only species **1** and **2** absorb light at the excitation wavelength λ_{ex}. $\epsilon_i(\lambda_{ex})$ denotes the molar absorption coefficient of species i at λ_{ex}. Photoexcitation creates the excited-state species **1*** and **2***, which can decay by fluorescence (F) and nonradiative (NR) processes. The composite rate constant for those processes is represented by k_{0i} ($=k_{Fi} + k_{NRi}$) for species i*. The excited-state association reaction of **1*** with M is described by rate constant k_{21}, while k_{12} stands for the rate constant of dissociation of **2*** into **1*** and M. The addition of the titrant M also accelerates the depopulation of the excited states by k_{q1}[M][**1***] and k_{q2}[M][**2***] for species **1*** and **2***, respectively, where k_{qi} stands for the Stern−Volmer rate constant of quenching of species i*. To summarize, in this report, we will explore the steady-state fluorescence of the photophysical system where the titrant M also acts as quencher of the excited-state species. It must be noted that this situation has one experimental variable less than the case where the concentrations of the quencher and titrant can be changed independently.[9]

Fluorometric titrations are constantly being used to determine K_d values of numerous different complexes. For example, Scheme 1 may depict the binding of an ion by a fluorescent ion indicator and the corresponding dissociation of the formed complex.[5,10−13] In that case, species **1** represents the free form of the fluorescent ion indicator, species **2** represents the corresponding bound form, and M stands for the ion. To illustrate the wide-ranging applicability of Scheme 1, we can refer to the formation of a well-defined 1:1 complex between glucose and a fluorescent bisboronic acid sensor at neutral pH,[14] the pK_a determination of pH indicators,[10,15−17] the binding of cellular retinoic acid binding proteins to all-*trans*-retinoic acid, acitretin, and 9-*cis*-retinoic acid,[18] the 1:1 binding of an inhibitor to milk xanthine oxidase,[19] and the binding of chromogranin A to calmodulin in the presence and absence of Ca^{2+},[20] to name just a few.

In Scheme 1, the steady-state fluorescence signal $F(\lambda_{ex},\lambda_{em},[M])$ measured at emission wavelength λ_{em} due to excitation at λ_{ex} is given by[1,8]

$$F(\lambda_{ex},\lambda_{em},[M]) = -\zeta(\lambda_{em})\mathbf{c}(\lambda_{em})\mathbf{A}^{-1}\mathbf{b}(\lambda_{ex},[M]) \quad (1)$$

where $\zeta(\lambda_{em})$ is an instrumental factor. $\mathbf{c}(\lambda_{em})$ is the 1×2 row vector of the emission weighting factors $c_i(\lambda_{em})$ (eq 2).[8] k_{Fi} is

$$c_i(\lambda_{em}) = k_{Fi}\int_{\Delta\lambda_{em}} \rho_i(\lambda_{em})\, d\lambda_{em} \quad (2)$$

the fluorescence rate constant of species i*; $\Delta\lambda_{em}$ is the emission wavelength interval around λ_{em} where the fluorescence signal is monitored; and $\rho_i(\lambda_{em})$ is the spectral emission density of species i* at λ_{em}.[8]

$\mathbf{A}$ is the 2×2 matrix defined by eq 3,[8] and $\mathbf{A}^{-1}$ is its inverse.

$$\mathbf{A} = \begin{bmatrix} -(k_{01} + [k_{21} + k_{q1}][M]) & k_{12} \\ k_{21}[M] & -(k_{02} + k_{12} + k_{q2}[M]) \end{bmatrix} \quad (3)$$

$\mathbf{b}(\lambda_{ex},[M])$ is the 2×1 column vector of the zero-time concentrations [i*](0). If Beer's law is obeyed and if the absorbance of species i is low (<0.1), then the elements $b_i(\lambda_{ex},[M])$ of $\mathbf{b}(\lambda_{ex},[M])$ can be approximated as[1]

$$b_i(\lambda_{ex},[M]) \approx 2.3d\epsilon_i(\lambda_{ex})[i]I_0(\lambda_{ex}) \quad (4)$$

where d stands for the excitation light path and $I_0(\lambda_{ex})$ represents the light flux at λ_{ex} impinging on the sample.

Expressing the ground-state dissociation constant K_d in the form of molar concentrations

$$K_d = [\mathbf{1}][M]/[\mathbf{2}] \quad (5)$$

and substituting eqs 3−5 into eq 1 yields

$$F(\lambda_{ex},\lambda_{em},[M]) = \frac{F(\lambda_{ex},\lambda_{em},[M])}{\psi(\lambda_{ex},\lambda_{em})} = \frac{a_1(\lambda_{em},[M])\epsilon_1(\lambda_{ex})K_d + a_2(\lambda_{em},[M])\epsilon_2(\lambda_{ex})[M]}{K_d + [M]} \quad (6)$$

with

$$\psi(\lambda_{ex},\lambda_{em}) = 2.3d\zeta(\lambda_{em})I_0(\lambda_{ex})([\mathbf{1}] + [\mathbf{2}]) \quad (7)$$

and $a_i(\lambda_{em}, [M])$ ($i = 1, 2$) defined by eqs 8a−c.

$$a_1(\lambda_{em},[M]) = \{c_1(\lambda_{em})(k_{02} + k_{12}) + [c_1(\lambda_{em})k_{q2} + c_2(\lambda_{em})k_{21}][M]\}/\alpha([M]) \quad (8a)$$

$$a_2(\lambda_{em},[M]) = \{c_1(\lambda_{em})k_{12} + c_2(\lambda_{em})k_{01} + c_2(\lambda_{em})(k_{21} + k_{q1})[M]\}/\alpha([M]) \quad (8b)$$

$$\alpha([M]) = k_{01}(k_{02} + k_{12}) + [k_{01}k_{q2} + k_{02}k_{21} + k_{q1}(k_{02} + k_{12})][M] + k_{q2}(k_{21} + k_{q1})[M]^2 \quad (8c)$$

3. Estimation of K_d

3.1. Direct Parametric Fit of the Fluorometric Titration Curves. Substituting eqs 8a−c into eq 6 yields

$$F(\lambda_{ex},\lambda_{em},[M]) = \frac{y_0(\lambda_{ex},\lambda_{em}) + y_1(\lambda_{ex},\lambda_{em})[M] + y_2(\lambda_{ex},\lambda_{em})[M]^2}{1 + x_1[M] + x_2[M]^2 + x_3[M]^3} \quad (9)$$

with

$$y_0(\lambda_{ex},\lambda_{em}) = \frac{\epsilon_1(\lambda_{ex})c_1(\lambda_{em})}{k_{01}} \quad (10a)$$

$$y_1(\lambda_{ex},\lambda_{em}) = \frac{\epsilon_1(\lambda_{ex})K_d\lfloor c_1(\lambda_{em})k_{q2} + c_2(\lambda_{em})k_{21}\rfloor + \epsilon_2(\lambda_{ex})[c_1(\lambda_{em})k_{12} + c_2(\lambda_{em})k_{01}]}{K_d k_{01}(k_{02} + k_{12})} \quad (10b)$$

$$y_2(\lambda_{ex},\lambda_{em}) = \frac{\epsilon_2(\lambda_{ex})c_2(\lambda_{em})(k_{21} + k_{q1})}{K_d k_{01}(k_{02} + k_{12})} \quad (10c)$$

$$x_1 = \frac{k_{01}k_{q2} + k_{02}k_{21}}{k_{01}(k_{02} + k_{12})} + \frac{k_{01} + K_d k_{q1}}{K_d k_{01}} \quad (11a)$$

$$x_2 = \frac{k_{01}k_{q2} + k_{q1}k_{12} + (K_d k_{q2} + k_{02})(k_{21} + k_{q1})}{K_d k_{01}(k_{02} + k_{12})} \quad (11b)$$

$$x_3 = \frac{k_{q2}(k_{21} + k_{q1})}{K_d k_{01}(k_{02} + k_{12})} \quad (11c)$$

From eqs 9−11, it follows that the ground-state dissociation constant K_d, the rate constants $\{k_{01}, k_{02}, k_{12}, k_{21}, k_{q1}, k_{q2}\}$, the emission weighting factors $\{c_1(\lambda_{em}), c_2(\lambda_{em})\}$, and the molar absorption coefficients $\{\epsilon_1(\lambda_{ex}), \epsilon_2(\lambda_{ex})\}$ are accessible from the coefficients $y_k(\lambda_{ex},\lambda_{em})$ ($k = 0, 1, 2$) and x_k ($k = 1, 2, 3$), which can be obtained via direct parameter fit of the measured titration curve. Although nonlinear estimation of $\{y_k(\lambda_{ex},\lambda_{em})$ ($k = 0, 1, 2$), x_k ($k = 1, 2, 3$)$\}$ is possible (requiring initial guesses for all parameters), a simpler way of performing the analysis is by linearization of eq 9, yielding eq 12. The linear parameters

$$F(\lambda_{ex},\lambda_{em},[M]) + x_1F(\lambda_{ex},\lambda_{em},[M])[M] + x_2F(\lambda_{ex},\lambda_{em},[M])[M]^2 + x_3F(\lambda_{ex},\lambda_{em},[M])[M]^3 = y_0(\lambda_{ex},\lambda_{em}) + y_1(\lambda_{ex},\lambda_{em})[M] + y_2(\lambda_{ex},\lambda_{em})[M]^2 \quad (12)$$

$y_k(\lambda_{ex},\lambda_{em})$ ($k = 0, 1, 2$) and x_k ($k = 1, 2, 3$) in eq 12 can be estimated directly using linear least-squares minimization.

3.2. Identifiability. Obviously, the set of eqs 10 and11 does not supply the unique solution for the system parameters $\{K_d, k_{01}, k_{02}, k_{12}, k_{21}, k_{q1}, k_{q2}, c_1(\lambda_{em}), c_2(\lambda_{em}), \epsilon_1(\lambda_{ex}), \epsilon_2(\lambda_{ex})\}$. Consider, for example, the ground-state dissociation constant K_d, which is the parameter of primary interest in any fluorometric titration study. Combining eqs 11a−c yields a polynomial (eq 13).

$$x_3K_d^3 - x_2K_d^2 + x_1K_d - 1 = 0 \quad (13)$$

Using the symbolic mathematics program Maple V (Waterloo Maple Inc.; see Supporting Information), we obtain three roots for the polynomial of eq 13 ($k_{q2} \neq 0$):

$$\text{root}_1 = K_d \quad (14a)$$

$$\text{root}_{2,3} = \frac{k_{01}k_{q2} + k_{q1}k_{12} + k_{02}(k_{21} + k_{q1})}{2k_{q2}(k_{21} + k_{q1})} \pm \frac{\sqrt{(k_{01}k_{q2} - k_{q1}k_{12} - k_{02}(k_{21} + k_{q1}))^2 - 4k_{q2}k_{01}k_{12}k_{21}}}{2k_{q2}(k_{21} + k_{q1})} \quad (14b)$$

The values of $\text{root}_{2,3}$ defined by eq 14b are independent of K_d; therefore, if the true values of the rate constants are known a priori, the $\text{root}_{2,3}$ corresponding to the wrong values of K_d can be rejected. If the true values of rate constants are unknown, the correct selection of K_d requires additional information about the system under investigation.

In this section, we investigate whether K_d (as well as the other system parameters) can be uniquely determined by algebraic manipulations of the error-free coefficients $y_k(\lambda_{ex},\lambda_{em})$ ($k = 0$, 1, 2) and x_k ($k = 1, 2, 3$) at different λ_{ex} and λ_{em}. Because the coefficients $\{y_k(\lambda_{ex},\lambda_{em})$ ($k = 0, 1, 2$), x_k ($k = 1, 2, 3$)$\}$ can be uniquely determined via direct parameter fit of a single titration curve (see eqs 9 and 12), the aim of the identifiability analysis is to verify if one can find alternative parameter sets, say $\{K_d^+, k_{01}^+, k_{02}^+, k_{12}^+, k_{21}^+, k_{q1}^+, k_{q2}^+, c_1^+(\lambda_{em}), c_2^+(\lambda_{em}), \epsilon_1^+(\lambda_{ex}), \epsilon_2^+(\lambda_{ex})\}$ in addition to the true set $\{K_d, k_{01}, k_{02}, k_{12}, k_{21}, k_{q1}, k_{q2}, c_1(\lambda_{em}), c_2(\lambda_{em}), \epsilon_1(\lambda_{ex}), \epsilon_2(\lambda_{ex})\}$, that satisfy the following set of equations based on y_k ($k = 0, 1, 2$) (eqs 10a−10c).

$$\frac{\epsilon_1(\lambda_{ex})c_1(\lambda_{em})}{k_{01}} = \frac{\epsilon_1^+(\lambda_{ex})c_1^+(\lambda_{em})}{k_{01}^+} \quad (15a)$$

$$\frac{\epsilon_1(\lambda_{ex})K_d\lfloor c_1(\lambda_{em})k_{q2} + c_2(\lambda_{em})k_{21}\rfloor + \epsilon_2(\lambda_{ex})[c_1(\lambda_{em})k_{12} + c_2(\lambda_{em})k_{01}]}{K_d k_{01}(k_{02} + k_{12})} = \frac{\epsilon_1^+(\lambda_{ex})K_d^+[c_1^+(\lambda_{em})k_{q2}^+ + c_2^+(\lambda_{em})k_{21}^+] + \epsilon_2^+(\lambda_{ex})[c_1^+(\lambda_{em})k_{12}^+ + c_2^+(\lambda_{em})k_{01}^+]}{K_d^+ k_{01}^+(k_{02}^+ + k_{12}^+)} \quad (15b)$$

$$\frac{\epsilon_2(\lambda_{ex})c_2(\lambda_{em})(k_{21} + k_{q1})}{K_d k_{01}(k_{02} + k_{12})} = \frac{\epsilon_2^+(\lambda_{ex})c_2^+(\lambda_{em})(k_{21}^+ + k_{q1}^+)}{K_d^+ k_{01}^+(k_{02}^+ + k_{12}^+)} \quad (15c)$$

A set of equations analogous to eqs 15a−c can be constructed for each distinct λ_{ex} and λ_{em}. The set of identifiability equations should be supplemented by the equations for the coefficients x_k ($k = 1, 2, 3$) (eqs 11a−c), which are independent of λ_{ex} and λ_{em}:

$$\frac{k_{01}k_{q2} + k_{02}k_{21}}{k_{01}(k_{02} + k_{12})} + \frac{k_{01} + K_d k_{q1}}{K_d k_{01}} = \frac{k_{01}^+ k_{q2}^+ + k_{02}^+ k_{21}^+}{k_{01}^+(k_{02}^+ + k_{12}^+)} + \frac{k_{01}^+ + K_d^+ k_{q1}^+}{K_d^+ k_{01}^+} \quad (16a)$$

$$\frac{k_{01}k_{q2} + k_{q1}k_{12} + (K_d k_{q2} + k_{02})(k_{21} + k_{q1})}{K_d k_{01}(k_{02} + k_{12})} = \frac{k_{01}^+ k_{q2}^+ + k_{q1}^+ k_{12}^+ + (K_d^+ k_{q2}^+ + k_{02}^+)(k_{21}^+ + k_{q1}^+)}{K_d^+ k_{01}^+(k_{02}^+ + k_{12}^+)} \quad (16b)$$

$$\frac{k_{q2}(k_{21} + k_{q1})}{K_d k_{01}(k_{02} + k_{12})} = \frac{k_{q2}^+(k_{21}^+ + k_{q1}^+)}{K_d^+ k_{01}^+(k_{02}^+ + k_{12}^+)} \quad (16c)$$

Using the symbolic mathematics program Maple V (see Supporting Information), one finds that at least two excitation wavelengths [corresponding to different $\epsilon_1(\lambda_{ex})$, $\epsilon_2(\lambda_{ex})$] and two emission wavelengths [corresponding to different $c_1(\lambda_{em})$, $c_2(\lambda_{em})$] are required to have a unique solution for the admissible value K_d. Other system parameters cannot be uniquely determined, no matter how many titration curves (measured at different λ_{ex} and λ_{em}) are combined.

The solution of the identifiability problem immediately leads to the experimental design which will allow for the unique

determination of K_d. The explicit expression for K_d can be obtained using Maple V (see Supporting Information):

$$K_d = \frac{p_1^2 x_1 + p_1 p_2 x_2 + p_2^2 x_3 - p_1 p_3}{p_1^2 x_1^2 + (p_1 p_2 x_2 + p_2^2 x_3 - 2p_1 p_3)x_1 - p_2 p_3 x_2 + p_1 p_2 x_3 + p_3^2} \quad (17)$$

with

$$p_1 = z_{01} z_{11} - z_{02} z_{12} \quad (18a)$$

$$p_2 = (z_{02} - z_{01}) z_{12} z_{11} + z_{12} - z_{11} \quad (18b)$$

$$p_3 = (z_{11} - z_{12}) z_{01} z_{02} - z_{02} + z_{01} \quad (18c)$$

and

$$z_{0j} = \{y_2(\lambda_{ex}^j,\lambda_{em}^1) y_1(\lambda_{ex}^j,\lambda_{em}^2) - y_2(\lambda_{ex}^j,\lambda_{em}^2) y_1(\lambda_{ex}^j,\lambda_{em}^1)\}/D_j, \quad j = 1,2 \quad (19a)$$

$$z_{1j} = \{y_1(\lambda_{ex}^j,\lambda_{em}^1) y_0(\lambda_{ex}^j,\lambda_{em}^2) - y_1(\lambda_{ex}^j,\lambda_{em}^2) y_0(\lambda_{ex}^j,\lambda_{em}^1)\}/D_j, \quad j = 1,2 \quad (19b)$$

$$D_j = y_2(\lambda_{ex}^j,\lambda_{em}^1) y_0(\lambda_{ex}^j,\lambda_{em}^1) - y_2(\lambda_{ex}^j,\lambda_{em}^1) y_0(\lambda_{ex}^j,\lambda_{em}^1), \quad j = 1,2 \quad (19c)$$

where $y_k(\lambda_{ex}^j,\lambda_{em}^i)$, $k = 0, 1, 2$ are the coefficients obtained from the parameter fit of eq 9 to the experimental data measured at excitation wavelength λ_{ex}^j ($j = 1, 2$) and emission wavelength λ_{em}^i ($i = 1, 2$).

3.3. Model with Excited-State Association and without Quenching. In the absence of quenching ($k_{q1}[M] \approx 0$, $k_{q2}[M] \approx 0$), eq 9 simplifies to eq 20, with $y_0(\lambda_{ex},\lambda_{em})$ given by eq

$$F(\lambda_{ex},\lambda_{em},[M]) = \frac{y_0(\lambda_{ex},\lambda_{em}) + y_1(\lambda_{ex},\lambda_{em})[M] + y_2(\lambda_{ex},\lambda_{em})[M]^2}{1 + x_1[M] + x_2[M]^2} \quad (20)$$

10a. The coefficients y_k ($k = 1, 2$) and x_k ($k = 1, 2$) are given by eqs 21 and 22, respectively. Combining eqs 22a and 22b

$$y_1(\lambda_{ex},\lambda_{em}) = \frac{\epsilon_1(\lambda_{ex}) c_2(\lambda_{em}) K_d k_{21} + \epsilon_2(\lambda_{ex})[c_1(\lambda_{em}) k_{12} + c_2(\lambda_{em}) k_{01}]}{K_d k_{01}(k_{02} + k_{12})} \quad (21a)$$

$$y_2(\lambda_{ex},\lambda_{em}) = \frac{\epsilon_2(\lambda_{ex}) c_2(\lambda_{em}) k_{21}}{K_d k_{01}(k_{02} + k_{12})} \quad (21b)$$

$$x_1 = \frac{k_{21} k_{02}}{k_{01}(k_{02} + k_{12})} + \frac{1}{K_d} \quad (22a)$$

$$x_2 = \frac{k_{02} k_{21}}{K_d k_{01}(k_{02} + k_{12})} \quad (22b)$$

yields a polynomial (eq 23). This polynomial (eq 23) has two

$$x_2 K_d^2 - x_1 K_d + 1 = 0 \quad (23)$$

roots: one is the ground-state dissociation constant $root_1 = K_d$ and the other root is expressed as a function of the rate constants (eq 24).

$$root_2 = \frac{k_{01}(k_{02} + k_{12})}{k_{02} k_{21}} \quad (24)$$

Linear least-squares minimization as in section 3.1 gives estimates for the linear parameters $\{y_k(\lambda_{ex},\lambda_{em})$ ($k = 0, 1, 2$), x_k ($k = 1, 2$)$\}$. Analysis shows that without quenching the identifiability criteria for K_d remain the same: two excitation wavelengths λ_{ex}^j ($j = 1, 2$) and two emission wavelengths λ_{em}^i ($i = 1, 2$) are still necessary for the unique determination of K_d. The expression for the determination of K_d can be obtained from eq 25, which is obtained from eq 17 with $x_3 = 0$.

$$K_d = \frac{z_{01} z_{11} - z_{02} z_{12}}{(z_{01} z_{11} - z_{02} z_{12}) x_1 + z_{02} z_{01}(z_{12} - z_{11}) + z_{02} - z_{01}} \quad (25)$$

3.4. Model without Excited-State Association and without Quenching. Further simplification of eq 9 is possible if one can neglect the excited-state association ($k_{21}[M] \approx 0$) and quenching ($k_{q1}[M] \approx 0$, $k_{q2}[M] \approx 0$). Now eq 9 reduces to eq 26 with $y_0(\lambda_{ex},\lambda_{em})$ given by eq 10a. The coefficients $y_1(\lambda_{ex},\lambda_{em})$

$$F(\lambda_{ex},\lambda_{em},[M]) = \frac{F(\lambda_{ex},\lambda_{em},[M])}{\psi(\lambda_{ex},\lambda_{em})} = \frac{y_0(\lambda_{ex},\lambda_{em}) + y_1(\lambda_{ex},\lambda_{em})[M]}{1 + x_1[M]} \quad (26)$$

and x_1 are given by eqs 27 and 28, respectively.

$$y_1(\lambda_{ex},\lambda_{em}) = \frac{\epsilon_2(\lambda_{ex})[c_1(\lambda_{em}) k_{12} + c_2(\lambda_{em}) k_{01}]}{K_d k_{01}(k_{02} + k_{12})} \quad (27)$$

$$x_1 = 1/K_d \quad (28)$$

Equation 26 is equivalent with eq 6 with $a_i(\lambda_{em})$ ($i = 1, 2$) given by eqs 29a and 29b. It must be noted that $a_i(\lambda_{em})$ ($i = 1, 2$) are no longer dependent on [M]. In that case, $F(\lambda_{ex},\lambda_{em},[M])$ and $F(\lambda_{ex},\lambda_{em},[M])$ as a function of log[M] show a unique inflection point at $[M] = K_d$. The K_d value can be determined from[1]

$$a_1(\lambda_{em}) = c_1(\lambda_{em})/k_{01} \quad (29a)$$

$$a_2(\lambda_{em}) = \frac{c_1(\lambda_{em}) k_{12} + c_2(\lambda_{em}) k_{01}}{k_{01}(k_{02} + k_{12})} \quad (29b)$$

$$F(\lambda_{ex},\lambda_{em},[M]) = \frac{F_{max}(\lambda_{ex},\lambda_{em})[M] + F_{min}(\lambda_{ex},\lambda_{em}) K_d}{K_d + [M]} \quad (30)$$

by nonlinear fitting of eq 30 to the experimental fluorescence signals $F(\lambda_{ex},\lambda_{em},[M])$. $F_{min}(\lambda_{ex},\lambda_{em})$ and $F_{max}(\lambda_{ex},\lambda_{em})$ stand for the fluorescence signals at minimal and maximal [M], respectively (corresponding to the free (**1**) and bound (**2**) forms of the probe, respectively). This simple case has been treated adequately in the literature and will not be discussed further here.

4. Global Analysis of Computer-Generated Fluorometric Titration Curves

Here we explore by means of simulations the considered algorithms for the determination of the ground-state dissociation

constant K_d. It is obvious that the number of computer-generated photophysical systems (following the model depicted in Scheme 1) with different simulation values of the rate constants, the molar absorption coefficients ϵ_i, the emission weighting factors c_i, and the dissociation constant K_d is unlimited. Therefore, the presented examples serve only as an illustration of the global analysis method. The curve-fitting of a large range of computer-synthesized fluorometric titration curves corresponding to different simulation values is beyond the scope of this paper.

To simulate the first photophysical system, fluorometric titration curves were calculated according to eqs 9 and 20 using the K_d and rate constant values of the fluorescent K^+ indicator PBFI in aqueous solution:[21] $k_{01} = 1.1 \times 10^9$ s^{-1}, $k_{02} = 1.8 \times 10^9$ s^{-1}, $k_{12} = 1.37 \times 10^9$ s^{-1}, $k_{21} = 2.7 \times 10^8$ M^{-1} s^{-1}, $K_d = 6.62$ mM. The values of the quenching rate constants were chosen arbitrarily: $k_{q1} = (q)(4 \times 10^8$ M^{-1} s$^{-1})$ and $k_{q2} = (q)(2 \times 10^8$ M^{-1} s$^{-1})$, with q equal to 0 (no quenching), 1, 2, 5, or 10. Two combinations of the molar absorption coefficients ($\epsilon_1 = 28\,000$ M^{-1} cm^{-1}, $\epsilon_2 = 37\,300$ M^{-1} cm^{-1}, and $\epsilon_1 = 17\,000$ M^{-1} cm^{-1}, $\epsilon_2 = 42\,000$ M^{-1} cm^{-1}) and two combinations of relative emission weighting factors [$\tilde{c}_1 = c_1/(c_1 + c_2) = 0.37$, $\tilde{c}_2 = c_2/(c_1 + c_2) = 0.63$, and $\tilde{c}_1 = 0.63$, $\tilde{c}_2 = 0.37$] were used. The fluorescence data $F([M])$ calculated according to eq 20 (i.e., $q = 0$) for different combinations of $\{\epsilon_1, \epsilon_2, c_1, c_2\}$ as a function of $-\log[M]$ are shown in Figure 1a. Although the complicated dependence of $F([M])$ on [M] is evident from this figure, clear inflection points around 6.62 mM ($-\log[M] \approx 2.18$), corresponding to K_d, can be found. The associated fluorescence decay times $\tau_{S,L}([M])$ calculated as the negative reciprocals of the eigenvalues of matrix **A** (eq 3) are displayed in Figure 1b as a function of $-\log[M]$. Since $k_{01} < k_{02}$, for [M] $\rightarrow 0$, the short decay time τ_S reaches $1/(k_{02} + k_{12})$ whereas the long decay time τ_L equals $1/k_{01}$. For [M] $\rightarrow \infty$, τ_S always reaches zero while τ_L decreases to $1/k_{02}$ in the absence of quenching.[22] Importantly, the values of $\tau_{S,L}$ remain constant in the [M] range around K_d (=6.62 mM), indicating that in this concentration range the excited-state association is negligible.[4]

Figure 2a presents the fluorescence data $F([M])$ calculated according to eq 9 (for quenching with $q = 2$ in k_{q1} and k_{q2}) for different $\{\epsilon_1, \epsilon_2, c_1, c_2\}$ combinations as a function of $-\log[M]$. The effect of quenching is clearly visible at high [M], whereas at low [M] the curves are practically the same as in the absence of quenching (compare Figures 1a and 2a). The inflection point around K_d ($-\log[M] \approx 2.18$) is still visible. The associated decay times $\tau_{S,L}([M])$ are shown as a function of $-\log[M]$ in Figure 2b. At high [M] in the presence of quenching, both τ_S and τ_L asymptotically approach zero. At [M] around K_d, τ_S remains constant while τ_L starts decreasing at higher [M] (see Figures 1b and 2b). Obviously, the effect of [M] on the decay times becomes more pronounced when the quenching rate constants are higher.

To computer-generate the numerical fluorometric titration data (according to eqs 9 and 20), 12 [M] values (0.5 mM, 1 mM, 2 mM, 4 mM, 7 mM, 12 mM, 30 mM, 80 mM, 0.2 M, 0.4 M, 1 M, and 4 M) were used. As we have only 12 [M] values, each data point is very important and their selection is crucial. We have chosen the [M] values in such a way that they are approximately evenly distributed over the $-\log[M]$ scale from $\sim$3.30 to ~ -0.60.

Statistical noise, added to the simulated fluorescence titration curve, was described by Gaussian statistics, i.e., the final value of a fluorescence data point $F([M])$ of the titration curve at each concentration [M] is a Gaussian random value, with a mean

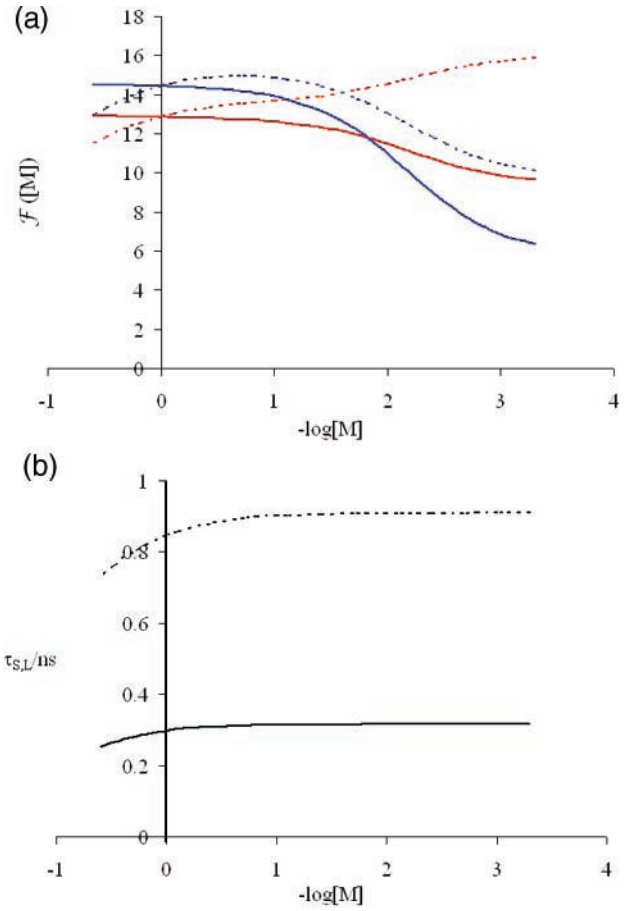

Figure 1. Photophysical system number 1: (a) fluorescence data $F([M])$ calculated according to eq 20 (without quenching) for different combinations of $\{\epsilon_1, \epsilon_2, c_1, c_2\}$ as a function of $-\log[M]$. The simulated rate constant and K_d values are $k_{01} = 1.1 \times 10^9$ s^{-1}, $k_{02} = 1.8 \times 10^9$ s^{-1}, $k_{12} = 1.37 \times 10^9$ s^{-1}, $k_{21} = 2.7 \times 10^8$ M^{-1} s^{-1}, $K_d = 6.62$ mM. Two combinations of the molar absorption coefficients [$\epsilon_1 = 28\,000$ M^{-1} cm^{-1}, $\epsilon_2 = 37\,300$ M^{-1} cm^{-1} (red); $\epsilon_1 = 17\,000$ M^{-1} cm^{-1}, $\epsilon_2 = 42\,000$ M^{-1} cm^{-1} (blue)] and two combinations of relative emission weighting factors [$\tilde{c}_1 = c_1/(c_1 + c_2) = 0.37$, $\tilde{c}_2 = c_2/(c_1 + c_2) = 0.63$ (solid lines); $\tilde{c}_1 = 0.63$, $\tilde{c}_2 = 0.37$ (dashed lines)] were used. (b) Associated τ_S (solid line) and τ_L (dashed line) as a function of $-\log[M]$, calculated with the rate constant values of Figure 1a.

equal to the exact value for this concentration and a standard uncertainty[23] defined by

$$u\{F([M]_i)\} = F([M]_i)/\Theta \tag{31}$$

where Θ is the signal-to-noise ratio. Four levels of signal-to-noise ratio Θ were used: 1000, 500, 200, and 50.

Curve fitting was performed in three steps: (1) The linear least-squares algorithm was applied to eq 12 to generate initial guesses for the coefficients $\{y_k(\lambda^i_{ex},\lambda^j_{em})$, $(k = 0, 1, 2; i, j = 1, 2)$, x_k $(k = 1, 2, 3)\}$. (2) The final estimates for $y_k(\lambda^i_{ex},\lambda^j_{em})$ and x_k were obtained from the iterative nonlinear least-squares fitting of eq 9 to the experimental titration curves. (3) The obtained coefficients $y_k(\lambda^i_{ex},\lambda^j_{em})$ and x_k were further used for the calculation of K_d according to eq 17.

Note that in steps 1 and 2, the parameters were obtained from global analysis of four titration curves [two emission wavelengths λ^i_{em} $(i = 1, 2)$ and two excitation wavelengths λ^j_{ex} $(j = 1, 2)$]. The parameters x_k (eq 11), being rational functions of the rate constants, independent of the emission or excitation wavelengths, were linked in the global analysis.

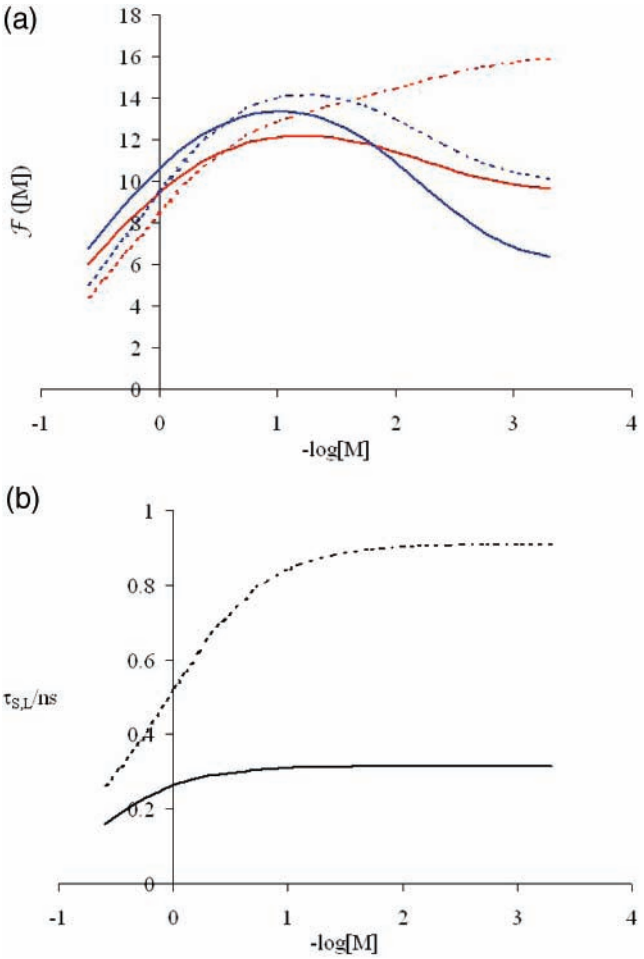

Figure 2. Photophysical system number 1: (a) fluorescence data $F([M])$ calculated according to eq 9 (with quenching) for different combinations of $\{\epsilon_1, \epsilon_2, c_1, c_2\}$ as a function of $-\log[M]$. The simulation values of rate constants, molar absorption coefficients ϵ_i, relative emission weighting factors $\tilde{c}_i$, and K_d are those of Figure 1. The simulated quenching rate constants are $k_{q1} = 8 \times 10^8$ M^{-1} s^{-1} and $k_{q2} = 4 \times 10^8$ M^{-1} s^{-1}. (b) Associated τ_S (solid line) and τ_L (dashed line) as a function of $-\log[M]$, calculated with the rate constant values of Figures 1 and 2a.

This algorithm can also be applied to the model without quenching by fixing the quenching rate constants k_{q1} and k_{q2} to 0 (see also eqs 20 and 25).

For each set of system parameters, 100 simulated titration curves were generated, each one with a different realization of statistical noise. The values of K_d were estimated from the 100 computer-generated titration curves, and the estimates were stored for the calculation of the mean value μ,

$$\mu\{K_d\} = \sum_{n=1}^{100} K_d^n/100 \tag{32}$$

and the variance u^2,

$$u^2\{K_d\} = \sum_{n=1}^{100} (K_d^n)^2/100 - \mu\{K_d\}^2 \tag{33}$$

where K_d^n is the estimator of K_d obtained in run n.

The results of the analyses of the simulated fluorometric data of this photophysical system are compiled in Table 1. It is evident that K_d is always estimated most accurately for higher signal-to-noise ratios ($\Theta = 500, 1000$). Low Θ levels (50, 200) lead to inaccurate K_d values, especially if the quenching is more pronounced ($q = 5, 10$). In these cases (i.e., low Θ combined with high q) the standard uncertainties $u\{K_d\}$ also are large. For higher Θ levels (500, 1000), the standard uncertainty $u\{K_d\}$ is the lowest for the systems without quenching ($q = 0$) and those with moderate quenching ($q = 1, 2$). Increase of the quenching rate constants k_{q1} and k_{q2} (by increasing q from 1 to 10) leads to a more rapid decay of the titration curve at higher [M] and less accurate and less precise K_d estimates.

TABLE 1: Photophysical System Number 1, Mean Value (μ) and Corresponding Standard Uncertainty (u) of the Estimated Values of K_d by Global Analysis of Four Fluorometric Titration Curves Synthesized According to the Models Described by Eq 9 (with Excited-State Association and Quenching) and Eq 20 (with Excited-State Association and without Quenching) for Two Combinations of the Molar Absorption Coefficients and Two Combinations of the Relative Emission Weighting Factors[a]

			Θ			
quenching	fitting model	estimator	1000	500	200	50
$q = 0$ (no quenching)	eq 20	$\mu\{K_d\}$	6.61	6.60	6.55	6.49
		$u\{K_d\}$	0.077	0.15	0.44	2.47
$q = 1$	eq 9	$\mu\{K_d\}$	6.62	6.62	6.56	5.83
		$u\{K_d\}$	0.034	0.068	0.64	2.62
$q = 2$	eq 9	$\mu\{K_d\}$	6.61	6.62	6.69	6.34
		$u\{K_d\}$	0.032	0.072	0.83	2.81
$q = 5$	eq 9	$\mu\{K_d\}$	6.62	6.64	7.21	4.48
		$u\{K_d\}$	0.15	0.27	1.18	8.34
$q = 10$	eq 9	$\mu\{K_d\}$	6.65	6.60	5.66	8.24
		$u\{K_d\}$	0.32	1.60	6.33	9.16

[a] $\epsilon_1 = 28\,000$ M^{-1} cm^{-1}, $\epsilon_2 = 37\,300$ M^{-1} cm^{-1} and $\epsilon_1 = 17\,000$ M^{-1} cm^{-1}, $\epsilon_2 = 42\,000$ M^{-1} cm^{-1}. $\tilde{c}_1 = 0.37$, $\tilde{c}_2 = 0.63$ and $\tilde{c}_1 = 0.63$, $\tilde{c}_2 = 0.37$. The following values of the model parameters were used: $K_d = 6.62$ mM, $k_{01} = 1.1 \times 10^9$ s^{-1}, $k_{02} = 1.8 \times 10^9$ s^{-1}, $k_{12} = 1.37 \times 10^9$ s^{-1}, $k_{21} = 2.7 \times 10^8$ M^{-1} s^{-1}, $k_{q1} = (q)(4 \times 10^8$ M^{-1} $s^{-1})$, and $k_{q2} = (q)(2 \times 10^8$ M^{-1} $s^{-1})$.

To check the generality of the results of this analysis, a second photophysical system was simulated with $k_{01} > k_{02}$ (in contrast to the previous photophysical system) and a much larger value for the excited-state association rate constant k_{21}. Contrary to the first system, the relation $k_{01} > k_{02}$ leads to a different pattern for τ_L at high [M] in the absence of quenching.[22] Indeed, τ_L increases with increasing [M] to reach $1/k_{02}$ for $[M] \rightarrow \infty$. For $[M] \rightarrow 0$ and if $k_{01} < k_{02} + k_{12}$ (as is the case here) we have $\tau_L = 1/k_{01}$ and $\tau_S = 1/(k_{02} + k_{12})$.[22] The values of the quenching rate constants $\{k_{q1}, k_{q2}\}$, the molar absorption coefficients $\{\epsilon_1, \epsilon_2\}$, the relative emission weighting factors $\{\tilde{c}_1\}$, and the dissociation constant K_d (=6.62 mM) are the same as for the first photophysical system. The simulation excited-state deactivation/exchange rate constant values are: $k_{01} = 1.8 \times 10^8$ s^{-1}, $k_{02} = 1.7 \times 10^8$ s^{-1}, $k_{12} = 1.1 \times 10^8$ s^{-1}, $k_{21} = 5 \times 10^{10}$ M^{-1} s^{-1} (i.e., $k_{01} > k_{02}$ and $k_{01} < k_{02} + k_{12}$). The higher value for k_{21} (compared to the previous system) makes the excited-state association more prominent at lower [M]. Now changes of $F([M])$ are observed in the [M] range where values of $\tau_{S,L}$ vary.

Figure 3a show the fluorescence data $F([M])$ calculated according to eq 9 (for quenching with $q = 1$ in k_{q1} and k_{q2}) for different $\{\epsilon_1, \epsilon_2, c_1, c_2\}$ combinations as a function of $-\log[M]$. The effect of quenching is clearly visible at high [M], obscuring somewhat the inflection point around K_d. The corresponding decay times $\tau_{S,L}([M])$ as a function of $-\log [M]$ are shown in Figure 3b. At high [M], both τ_S and τ_L asymptotically approach 0. Both τ_S and τ_L vary in the [M] range

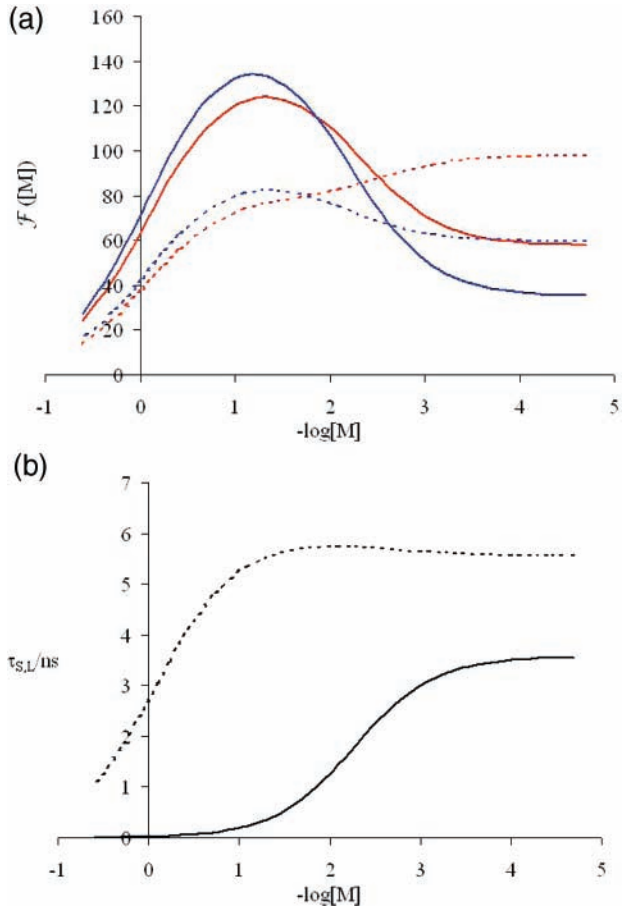

Figure 3. Photophysical system number 2: (a) fluorescence data $F([M])$ calculated according to eq 9 (with quenching) for different combinations of $\{\epsilon_1, \epsilon_2, c_1, c_2\}$ as a function of $-\log[M]$. Simulation values of rate constants and K_d are $k_{01} = 1.8 \times 10^8$ s^{-1}, $k_{02} = 1.7 \times 10^8$ s^{-1}, $k_{12} = 1.1 \times 10^8$ s^{-1}, $k_{21} = 5 \times 10^{10}$ M^{-1} s^{-1}, $k_{q1} = 8 \times 10^8$ M^{-1} s^{-1}, $k_{q2} = 4 \times 10^8$ M^{-1} s^{-1}, $K_d = 6.62$ mM. The molar absorption coefficients and the relative emission weighting factors are the same as for photophysical system number 1. Two combinations of the molar absorption coefficients [$\epsilon_1 = 28\,000$ M^{-1} cm^{-1}, $\epsilon_2 = 37\,300$ M^{-1} cm^{-1} (red); $\epsilon_1 = 17\,000$ M^{-1} cm^{-1}, $\epsilon_2 = 42\,000$ M^{-1} cm^{-1} (blue)] and two combinations of relative emission weighting factors [$\tilde{c}_1 = c_1/(c_1 + c_2) = 0.37$, $\tilde{c}_2 = c_2/(c_1 + c_2) = 0.63$ (solid lines); $\tilde{c}_1 = 0.63$, $\tilde{c}_2 = 0.37$ (dashed lines)] were used. (b) Corresponding τ_S (solid line) and τ_L (dashed line) values as a function of $-\log[M]$, calculated with the rate constant values of Figure 3a.

around K_d. The long decay time τ_L rises from $1/k_{01}$ at $[M] \approx 0$ with increasing [M] and subsequently drops to zero when $[M] \rightarrow \infty$.

Twelve [M] values (0.1 mM, 0.8 mM, 2 mM, 6 mM, 8 mM, 10 mM, 15 mM, 20 mM, 50 mM, 80 mM, 0.2 M, 0.6 M) were used to simulate the data points $F([M])$ at each concentration [M]. The choice of the [M] values covers the $-\log[M]$ range from 4.00 to ~0.22. The results of the analyses of the simulated fluorometric data of the second photophysical system are presented in Table 2. These results confirm the general tendencies in statistical characteristics of the K_d estimates observed for system number 1. However, there are two notable differences. First, the K_d estimates are more uncertain (larger u) at all signal-to-noise levels and quenching rates, proving that this system is more difficult to analyze. Second, system number 2 demonstrates better relative robustness with respect to quenching. For example, a 10-fold increase of the quenching rate constants (from $q = 1$ to 10) results in an almost 10-fold increase (at $\Theta = 1000$) of the uncertainty $u\{K_d\}$ in system number 1, whereas for system number 2, the same increase of

TABLE 2: Photophysical System Number 2, Mean Value (μ) and Corresponding Standard Uncertainty (u) of the Estimated Values of K_d by Global Analysis of Four Fluorometric Titration Curves Synthesized According to the Models Described by Eq 9 (with Excited-State Association and Quenching) and Eq 20 (with Excited-State Association and without Quenching)[a]

			Θ			
quenching	fitting model	estimator	1000	500	200	50
$q = 0$ (no quenching)	eq 20	$\mu\{K_d\}$	6.62	6.64	7.00	3.80
		$u\{K_d\}$	0.18	0.40	2.45	8.30
$q = 1$	eq 9	$\mu\{K_d\}$	6.64	6.70	6.80	3.83
		$u\{K_d\}$	0.22	0.47	3.55	10.6
$q = 2$	eq 9	$\mu\{K_d\}$	6.64	6.72	6.75	2.00
		$u\{K_d\}$	0.23	0.53	4.22	13.5
$q = 5$	eq 9	$\mu\{K_d\}$	6.65	6.74	7.46	6.31
		$u\{K_d\}$	0.28	0.66	4.41	15.3
$q = 10$	eq 9	$\mu\{K_d\}$	6.65	6.79	7.72	1.03
		$u\{K_d\}$	0.35	0.88	4.64	17.8

[a] $\epsilon_1 = 28\,000$ M^{-1} cm^{-1}, $\epsilon_2 = 37\,300$ M^{-1} cm^{-1} and $\epsilon_1 = 17\,000$ M^{-1} cm^{-1}, $\epsilon_2 = 42\,000$ M^{-1} cm^{-1}. $\tilde{c}_1 = 0.37$, $\tilde{c}_2 = 0.63$ and $\tilde{c}_1 = 0.63$, $\tilde{c}_2 = 0.37$. The following values of the model parameters were used: $K_d = 6.62$ mM, $k_{01} = 1.8 \times 10^8$ s^{-1}, $k_{02} = 1.7 \times 10^8$ s^{-1}, $k_{12} = 1.1 \times 10^8$ s^{-1}, $k_{21} = 5 \times 10^{10}$ M^{-1} s^{-1}, $k_{q1} = (q)(4 \times 10^8$ M^{-1} s$^{-1})$, and $k_{q2} = (q)(2 \times 10^8$ M^{-1} s$^{-1})$.

$\{k_{q1}, k_{q2}\}$ results in less than a 2-fold increase in uncertainty. This can be tentatively accounted for by the fact that for the first system we used the concentration scale up to 4 M (notably, points 1 and 4 M), and for the second system, the concentration scale is limited by 0.6 M. Therefore, in the latter case the effect of elevated quenching should be less pronounced. The general conclusion that low signal-to-noise ratios, Θ, and high quenching rates are detrimental to the accuracy and precision of the K_d estimates remains valid.

5. Conclusion

In this paper, we have shown that in the presence of excited-state association and quenching, the unique value of K_d can be obtained from global analysis of four fluorometric titration curves measured at two excitation wavelengths [corresponding to different $\epsilon_1(\lambda_{ex})$, $\epsilon_2(\lambda_{ex})$] and two emission wavelengths [corresponding to different $c_1(\lambda_{em})$, $c_2(\lambda_{em})$]. The other system parameters (rate constants, molar absorption coefficients, and emission weighting factors) cannot be uniquely determined no matter how many titration curves (measured at different wavelengths of excitation and emission) are combined. The results of global analyses of computer-generated fluorescence titration curves indicate that high signal-to-noise ratios and minimal quenching are favorable for the accurate and precise estimation of K_d.

Supporting Information Available: Maple scripts for (i) ground-state dissociation constant K_d from a single fluorometric titration curve (eq 14); (ii) identifiability of the ground-state dissociation constant K_d; and (iii) determination of the ground-state dissociation constant K_d (eqs 17 and 25). This material is available free of charge via the Internet at http://pubs.acs.org.

References and Notes

(1) Kowalczyk, A.; Boens, N.; Van den Bergh, V.; De Schryver, F. C. *J. Phys. Chem.* **1994**, *98*, 8585.

(2) Lakowicz, J. R. *Principles of Fluorescence Spectroscopy*, 3rd ed.; Springer-Verlag: New York, 2006.

(3) Valeur, B. *Molecular Fluorescence. Principles and Applications*; Wiley-VCH: Weinheim, Germany, 2002.

(4) Kowalczyk, A.; Boens, N.; Meuwis, K.; Ameloot, M. *Anal. Biochem.* **1997**, *245*, 28.

(5) Grynkiewicz, G.; Poenie, M.; Tsien, R. Y. *J. Biol. Chem.* **1985**, *260*, 3440.

(6) This term is usually employed with reference to a set of absorption spectra plotted on the same chart for a set of solutions in which the sum of the concentrations of two principal absorbing components, A and B, is constant. The curves of absorbance against wavelength (or frequency) for such a set of mixtures often all intersect at one or more points, called isosbestic points (http://www.iupac.org/goldbook/I03310.pdf).

Wavelength, wavenumber, or frequency at which the total absorbance of a sample does not change during a chemical reaction or a physical change of the sample (Braslavsky, S. E. *Glossary of Terms Used in Photochemistry* (IUPAC Recommendations 2006), 3rd ed.; *Pure Appl. Chem.* **2007**, *79*, 293.

(7) Novikov, E.; Stobiecka, A.; Boens, N. *J. Phys. Chem. A* **2000**, *104*, 5388.

(8) Ameloot, M.; Boens, N.; Andriessen, R.; Van den Bergh, V.; De Schryver, F. C. *J. Phys. Chem.* **1991**, *95*, 2041.

(9) Andriessen, R.; Ameloot, M.; Boens, N.; De Schryver, F. C. *J. Phys. Chem.* **1992**, *96*, 314.

(10) Haugland, R. P. *The Handbook. A Guide to Fluorescent Probes and Labeling Technologies*, 10th ed.; Molecular Probes: Eugene, OR, 2005.

(11) Basarić, N.; Baruah, M.; Qin, W.; Metten, B.; Smet, M.; Dehaen, W.; Boens, N. *Org. Biomol. Chem.* **2005**, *3*, 2755.

(12) Baruah, M.; Qin, W.; Vallée, R. A. L.; Beljonne, D.; Rohand, T.; Dehaen, W.; Boens, N. *Org. Lett.* **2005**, *7*, 4377.

(13) Yu, Y.; Lin, L.-R.; Yang, K.-B.; Zhong, X.; Huang, R.-B.; Zheng, L.-S *Talanta* **2006**, *69*, 103.

(14) Eggert, H.; Frederiksen, J.; Morin, C.; Norrild, J. C. *J. Org. Chem.* **1999**, *64*, 3846.

(15) Petrov, J. G.; Möbius, D. *Langmuir* **1989**, *5*, 523.

(16) Qin, W.; Baruah, M.; De Borggraeve, W. M.; Boens, N. *J. Photochem. Photobiol., A* **2006**, *183*, 190.

(17) Baruah, M.; Qin, W.; Basarić, N.; De Borggraeve, W. M.; Boens, N. *J. Org. Chem.* **2005**, *70*, 4152.

(18) Norris, A. W.; Cheng, L.; Giguère, V.; Rosenberger, M.; Li, E. *Biochim. Biophys. Acta* **1994**, *1209*, 10.

(19) Okamoto, K.; Nishino, T. *J. Biol. Chem.* **1995**, *270*, 7816.

(20) Yoo, S. H. *Biochemistry* **1992**, *31*, 6134.

(21) Meuwis, K.; Boens, N.; De Schryver, F. C.; Gallay, J.; Vincent, M. *Biophys. J.* **1995**, *68*, 2469.

(22) Van den Bergh, V.; Kowalczyk, A.; Boens, N.; De Schryver, F. C. *J. Phys. Chem.* **1994**, *98*, 9503.

(23) According to ISO [*Guide to the Expression of Uncertainty in Measurement (GUM)*, 1st ed.; International Organization for Standardization (ISO): Geneva, Switzerland, 1995; ISBN 92-67-10188-9. Taylor, B. N.; Kuyatt, C. E. *Guidelines for Evaluating and Expressing Uncertainty of NIST Measurement Results*; NIST Technical Note 1297; National Institute of Standards and Technology: Gaithersburg, MD, 1994.], the estimated standard deviation s evaluated by statistical methods should be termed standard uncertainty with suggested symbol u (i.e., $u = s$) and is equal to the positive square root of the estimated variance u^2.